Pharmacophore Fragment-Based Prediction and Gas-Phase ab Initio Optimization of Carvedilol Conformations

David R. P. Almeida,*,†,‡ Donna M. Gasparro,† Ferenc Fülöp,‡ and Imre G. Csizmadia†,§

Department of Chemistry, Lash Miller Laboratories, University of Toronto, 80 St. George Street, Toronto, Ontario, Canada M5S 3H6, Institute of Pharmaceutical Chemistry, University of Szeged, 6720 Szeged, Eotvos u. 6, Hungary, and Department of Medicinal Chemistry, University of Szeged, Dom ter 8, 6720 Szeged, Hungary

Received: March 3, 2004; In Final Form: May 12, 2004

This current communication gives the results of a novel computational molecular method of selecting, from a vast number of possible conformations, the dominant low-energy states of a large molecule by dividing it into separately analyzable structure−activity fragments. Carvedilol is a cardiovascular drug of proven efficacy with multiple molecular targets: it acts as a nonselective β-adrenoceptor (β_1 and β_2) and selective α_1-adrenoceptor antagonist, an antioxidant able to reduce reactive oxygen species (ROS)-mediated oxidative stress, a beneficial modulator of cardiac electrophysiological properties (K^+ and Ca^{2+} ion channels), a multifaceted cardioprotector, and novel antifibrillar agent able to inhibit amyloid-beta (Aβ) fibril formation. Given carvedilol's varied pharmacodynamic profiles, and the fact that a thorough analysis of its potential energy hypersurface (PEHS) has not yet been performed, an original molecular fragmentation method was developed to reveal carvedilol's low-energy states, to divulge their relevance to its biological activity. Multidimensional conformational analysis (MDCA) leads to a total of 177 147 (3^{11}) conformational possibilities, whereas fragmentation studies predict 240 gas-phase conformations. Structural predictions were tested on protonated *R*-carvedilol with gas-phase molecular orbital (MO) computations of PEHS minima at the restricted Hartree−Fock (RHF) (RHF/3-21G) level of theory, using the Gaussian 98 software program. Computation of the 240 predicted (input) carvedilol conformations revealed 121 converged (i.e., fully optimized) structures, of which nine possessed a conformer relative energy of <4 kcal/mol. Seven of these nine conformers possess a unique "tetra-centric" (four-centered) spiro-type structure that is composed of two rings (six- and eight-membered) enclosed by two O···H−N hydrogen bonds (H-bonds) that are connected via the protonated N atom in the side chain of carvedilol; this conformation is largely determined by the carbazole-containing pharmacophore (Fragment A) of carvedilol. In regard to the utility of the rational molecular fragmentation method used to predict and optimize the carvedilol structures, it is determined that 8 of the 11 torsional angles were accurately predicted (72.7%), according to torsional angle conformation distribution. The strength of this fragmentation method relies on full MDCA optimization of the individual fragments, which are then used to predict the carvedilol conformations. As such, the predicted inputs possess an inherent degree of energy minimization and, thus, are able to provide a better hypothesis of relevant sections of the carvedilol surface versus a random sampling of the PEHS. The elucidation of carvedilol's conformational identity greatly aids the full molecular understanding of carvedilol's adrenoceptor binding structure and carvedilol's involvement, at the molecular level, in ameliorating pathological states such as oxidative stress and Alzheimer's disease.

1. Introduction

Carvedilol, 1-(9H-carbazol-4-yloxy)-3-[2-(2-methoxy-phenoxy)ethylamino]-2-propanol ($C_{24}H_{26}N_2O_4$), is a cardiovascular drug that possesses multiple modes of action and is used in the treatment of hypertension, ischemic heart disease (IHD), and congestive heart failure (CHF).[1,2] The major molecular targets of carvedilol include antagonist action at α_1, β_1, and β_2 membrane adrenoceptors; reduction of reactive oxygen species (ROS); and modulation of K^+ and Ca^{2+} ion channels.[1] Carvedilol provides hemodynamic benefits such as peripheral vasodilation and reduction in cardiac work from balanced nonselective β-receptor blockage (β_1 and β_2) and selective α_1-receptor blockage.[1−3] In regard to cardioprotection, carvedilol exerts anti-proliferative/anti-atherogenic, anti-hypertrophic, anti-ischemic, and anti-arrhythmic actions by means of antioxidant effects, the improvement of glucose and lipid metabolism, the modulation of neurohormonal factors (e.g., nitric oxides), and beneficial cardiac electrophysiological properties (reviewed in ref 1).

Another cardioprotective effect of carvedilol resides in its ability to protect mitochondria from oxidative stress by uncoupling oxidative phosphorylation via a weak protonophoretic (proton transfer) mechanism that involves the amino group ($pK_a = 7.9$) of its side chain.[4] It has been proposed that carvedilol's amino group decreases the mitochondrial electric potential by the following mechanism: carvedilol binds a proton in the

* Author to whom correspondence should be addressed. E-mail address: dalmeida@medscape.com.
† University of Toronto.
‡ Institute of Pharmaceutical Chemistry.
§ Department of Medicinal Chemistry.

10.1021/jp040196f CCC: $27.50
Published on Web 06/29/2004

cytosolic leaflet of the inner mitochondrial membrane (low pH mitochondrial intermembrane space), crosses the mitochondrial membrane in the positive protonated form (driven by its high lipid solubility and mitochondria pH gradient), releases the proton in the higher pH mitochondrial matrix, and then returns to the intermembrane space in the neutral deprotonated form; the process can then begin again.[4] This phenomenon, which is known as "mild uncoupling", occurs when a small decrease in mitochondrial electric potential induces a significant reduction in the ROS produced by the mitochondrial respiratory chain.[4−6]

It has been shown that carvedilol and its active hydroxylated analogues act as novel antifibrillar agents that are able to inhibit amyloid-beta (Aβ) fibril formation.[7] According to the amyloid cascade hypothesis of Alzheimer's disease (AD), the accumulation of Aβ in extracellular senile plaques (SPs) in brain tissue drives AD pathogenesis.[8] The culprits of these processes are Aβ peptides consisting of 42 or 43 amino acids (abbreviated as Aβ1−42), which are prone to aggregation, oligomerization, and deposition in diffuse plaques and cause progressive synaptic and neuritic injury.[8−10] Recently, it has been shown that Aβ oligomers (dimers, trimers, or higher oligomers), in the absence of monomers and amyloid fibrils, are the main neurotoxic component of AD.[10−13] Given the aforementioned discussion, as an antifibrillar agent, carvedilol may have uses in the prevention or slowing of AD pathology. The effectiveness of carvedilol's inhibition of Aβ fibril formation is due to three factors: (1) a central basic amino pharmacophore, (2) two cyclic hydrophobic ring centroids, and (3) the molecular flexibility to adopt a specific three-dimensional pharmacophore conformation.[7] Although these three factors are recognized, it is currently not known if carvedilol binds to Aβ monomers, dimers, or other oligomers[7] or what type of interaction occurs between carvedilol and the Aβ peptide(s).

Given the multifaceted nature of carvedilol, it is necessary to reveal its complete molecular identity and conformational profile as a means to fully divulge the structural properties of its adrenoceptor binding conformation and further clarify its function in hemodynamic and cardioprotective mechanisms. Similarly, to expound on carvedilol's role in antioxidant pathways, the uncoupling of oxidative phosphorylation in mitochondria, and with Aβ peptide(s) in AD, its conformational identity is required, because conformation is a fundamental component of all of these processes. However, given carvedilol's 11 associated torsional angles and 177 147 (3^{11}) conformational possibilities (each torsional angle can assume gauche plus ($g+$), anti (a), or gauche minus ($g-$) orientations), this task is exceptionally extensive (cf. Figure 1). To remedy this problem, we previously developed a method to fragment the three pharmacophores of carvedilol into three independent structure−activity molecular fragments (cf. Figure 2).[14] This has been done both as a prelude to the evaluation of the entire drug molecule and to assess the success of such a methodological approach, i.e., rational molecular fragmentation of structure−activity regions, such as pharmacophores, as a means to study large complex molecular systems in great detail.

Earlier, we investigated all three fragments exhaustively,[14−17] analyzed the chiral properties of carvedilol,[17] and optimized several hydrogen-bond (H-bond) intramolecular attractive forces (IMAFs) present in the carvedilol molecule.[18] In this study, the development of this methodology is continued through the use of previous results from the individual fragments to predict and subsequently optimize a comprehensive list of possible carvedilol conformations, based on low-energy fragment conformations. This is performed to determine the conformations of carvedilol

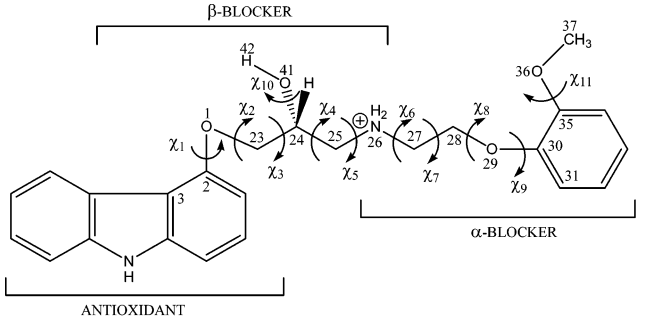

χ_1 = C23, O1, C2, C3
χ_2 = C24, C23, O1, C2
χ_3 = C25, C24, C23, O1
χ_4 = N26, C25, C24, C23
χ_5 = C27, N26, C25, C24
χ_6 = C28, C27, N26, C25
χ_7 = O29, C28, C27, N26
χ_8 = C30, O29, C28, C27
χ_9 = C31, C30, O29, C28
χ_{10} = H42, O41, C24, C23
χ_{11} = C37, O36, C35, C30

Figure 1. Molecular structure and pharmacophore structure−activity of N-protonated *R*-carvedilol and all torsional angle definitions used in the current study (numbers placed beside atoms were used to define all torsional angles for *R*-carvedilol in the z-matrix input for Gaussian 98).

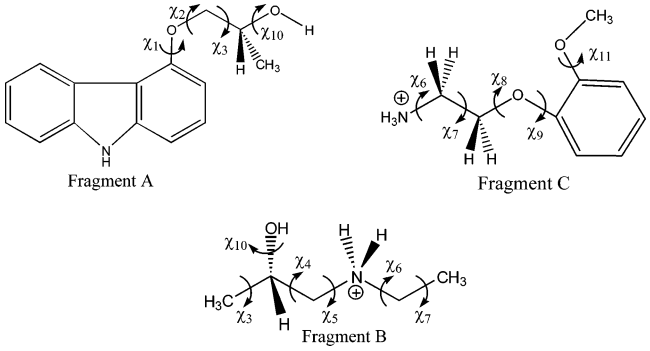

Figure 2. Carvedilol was divided into three molecular fragments based on pharmacophore structure−activity: *R*- and *S*-4-(2-hydroxypropoxy)-carbazol (Fragment A),[14,17] 2(*R* and *S*)-1-(ethylamonium)propane-2-ol (Fragment B),[15] and aminoethoxy-2-methoxy-benzene (Fragment C).[16] The results of *R*-Fragment A, *S*-Fragment B, and Fragment C (cf. Table 1) were used in this study to predict a comprehensive list of possible low-energy conformations for N-protonated carvedilol (*R*-configuration) (cf. Table S1). Predicted conformations were then subject to geometry optimization at the RHF/3-21G level of theory (cf. Table S2).

that are expected to dominate a gas-phase sample. Furthermore, these results highlight a novel computational approach, entitled rational molecular fragmentation, that allows selection, from a vast number of possible conformations, the dominant low-energy states of a complex molecular system by independently investigating pharmacophore fragments.

2. Methods

To allow explicit prediction and definition of conformation, a systematic numbering system has been used for all structures, such that corresponding torsional angles in the fragments (A, B, and C) and carvedilol are all defined in the same manner (cf. torsional angle definitions in Figure 1). Furthermore, conformational structural assignments for the conformational minima of a respective potential energy hypersurface (PEHS) are made according to eq 1:

$$\text{gauche plus } (g+) = 60.^\circ \text{ (ideal)} \pm 60^\circ \quad (1a)$$

$$\text{anti } (a) = 180.^\circ \text{ (ideal)} \pm 60^\circ \quad (1b)$$

$$\text{gauche minus } (g-) = -60.^\circ \text{ (ideal)} \pm 60^\circ \quad (1c)$$

Carvedilol is composed of three distinct pharmacophores (cf. Figures 1 and 2) and was thus divided into three molecular fragments, which were studied via multidimensional conformational analysis (MDCA): *R*- and *S*-4-(2-hydroxypropoxy)-carbazol (Fragment A) compounds possess the carbazole ring responsible for the direct antioxidant effects of carvedilol,[14,17] 2(*R* and *S*)-1-(ethylamonium)propane-2-ol (Fragment B) contains the protonophoretic amino group involved in the cardioprotective uncoupling of mitochondrial oxidative phosphorylation,[15] and aminoethoxy-2-methoxy-benzene (Fragment C) is the α_1-adrenergic antagonist pharmacophore of carvedilol.[16] The chiral parameters and interactions of Fragment A and carvedilol have also been described.[17]

The major H-bond IMAF of carvedilol has been shown to be an O1···H42−O41···H57 hydrogen bond motif initially found in Fragments A and B, along with a bifurcated intramolecular H-bond (O29···H46···O36, where H46 is an amine hydrogen) originally found in Fragment C (cf. ref 18 for specific structural information). Although some IMAFs of carvedilol have been evaluated,[18] this latter study addressed only a few conformations of carvedilol, whereas the current study analyzes a novel comprehensive list of possible carvedilol conformers not previously found in the literature. This comprehensive list is based on the MDCA results from the individual fragments as an attempt to arrive at the set of carvedilol's low-energy gas-phase conformations.

To ensure that all fragments correspond stereochemically with each other (i.e., torsional angle χ_{10} has the same orientation in all structures), only the B3LYP/6-31G(d) results of the *R*-configuration Fragment A PEHS (from ref 17), RHF/3-21G results of the *S*-configuration Fragment B PEHS (from ref 15), and RHF/3-21G results of the Fragment C PEHS (from ref 16) were used (cf. Figure 2). The selection criteria that has been applied utilizes all fragment geometries with a conformer relative energy of ≤2.00 kcal/mol from the individual PEHSs (cf. Table 1) as an attempt to predict only significantly populated, low-energy conformers of carvedilol. Continuing, the predictions were made for conformations of *R*-carvedilol only (cf. Figure 1). The PEHS conformers of carvedilol can be described by eq 2:

$$E = f(\chi_1, \chi_2, \chi_3, \chi_4, \chi_5, \chi_6, \chi_7, \chi_8, \chi_9, \chi_{10}, \chi_{11}) \quad (2)$$

The conformations of the low-energy converged fragment structures found in Table 1 were combined to create a maximum total of 240 distinct, nonredundant *R*-configuration carvedilol conformations (cf. Table S1 in the Supporting Information; note that Table S1 also displays the output-optimized torsional angle conformation if a structure successfully converged and may not be the same as the input conformation). The only incidence of overlapping, nonsymmetrical torsional angles between the three fragments was torsional angle χ_{10} in Fragments A and B (cf. Table 1); however, Fragments A and B only differed in their χ_{10} orientation in one conformation. Consequently, carvedilol predictions all possessed torsional angle χ_{10} in the $g+$ position, except for those combinations involving Fragment A conformation *aag*−*g*− (relative to torsional angles χ_1, χ_2, χ_3, and χ_{10}, respectively), which has resulting conformational predictions with torsional angle χ_{10} in the both the $g+$ and $g-$ positions (cf. Table S1). The total conformational combinations for

TABLE 1: Selected Optimized Fragment A, B, and C Conformers Used to Predict Low-Energy Carvedilol Conformations in This Study[a]

Fragment A, *R*-Configuration, B3LYP/6-31G(d) Results				
Converged Torsional Angle Conformation				relative energy (kcal/mol)
χ_1	χ_2	χ_3	χ_{10}	
a	*a*	*a*	*g*+	0.00
a	*a*	*g*−	*g*−	0.87
a	*g*−	*a*	*g*+	1.47
g−	*a*	*a*	*g*+	1.58
Fragment B, *S*-Configuration, RHF/3-21G Results				
Converged Torsional Angle Conformation				relative energy (kcal/mol)
χ_4	χ_5	χ_6	χ_{10}	
a	*a*	*a*	*g*+	0.00
a	*g*+	*a*	*g*+	0.36
a	*a*	*g*−	*g*+	0.63
g+	*a*	*a*	*g*+	0.66
a	*a*	*g*+	*g*+	1.17
a	*g*+	*g*+	*g*+	1.26
g+	*a*	*g*+	*g*+	1.28
g+	*a*	*g*−	*g*+	1.83
Fragment C, No Point Chirality, RHF/3-21G results				
Converged Torsional Angle Conformation				relative energy (kcal/mol)
χ_7	χ_8	χ_9	χ_{11}	
g+	*g*+	*g*+	*g*−	0.00
g−	*g*−	*g*−	*g*+	0.00
g+	*a*	*g*−	*a*	0.34
g−	*a*	*g*+	*a*	0.34
g+	*g*−	*g*−	*g*+	1.03
g−	*g*+	*g*+	*g*−	1.03

[a] Data for Fragment A were taken from ref 17, data for Fragment B were taken from ref 15, and data for Fragment C were taken from ref 16. All individual fragment structures with a conformer relative energy of ≤2.00 kcal/mol were deemed low-energy conformers and incorporated to generate the carvedilol conformations found in Table S1 of the Supporting Information (cf. Section 2, Methods).

R-configuration carvedilol with torsional angle χ_{10} in the $g+$ and $g-$ position are displayed in eqs 3 and 4, respectively. Thus, the total predicted number of unique carvedilol conformations based on the Fragment A, B, and C low-energy conformers in Table 1 is 240, which can be summed as follows: eq 3 ($\chi_{10} = g+$) + eq 4 ($\chi_{10} = g-$) = 192 ($\chi_{10} = g+$) + 48 ($\chi_{10} = g-$) = 240 (cf. Table S1). Finally, note that the six Fragment C conformations are not unique but rather are axis chiral pairs (see ref 17 for explanation); however, all were included in this study for completeness.

(4 Fragment A conformations) ×
(8 Fragment B conformations) ×
(6 Fragment C conformations) =
192 *R*-configuration carvedilol unique conformations
(All have torsional angle χ_{10} in the $g+$ position) (3)

(1 Fragment A conformation) ×
(8 Fragment B conformations) ×
(6 Fragment C conformations) =
48 *R*-configuration carvedilol unique conformations
(All have torsional angle χ_{10} in the $g-$ position) (4)

The conformational predictions for *R*-configuration carvedilol in Table S1 were tested with molecular orbital (MO) optimization of the PEHS conformational minima. Full geometry optimizations were performed in the gas phase ($\epsilon = 0.0$) on

TABLE 2: RHF/3-21G-Optimized Carvedilol Structures Identified as Gas-Phase Low-Energy Conformers Based on a Conformer Relative Energy of <4.00 kcal/mol (cf. Figures 3 and 4)

structure code	Torsional Angle (degrees)											energy (hartree)	relative energy (kcal/mol)
	χ_1	χ_2	χ_3	χ_4	χ_5	χ_6	χ_7	χ_8	χ_9	χ_{10}	χ_{11}		
C-*R*-246	107.18	−170.32	−52.20	67.57	88.63	−173.38	−49.09	−66.13	−69.97	70.21	83.62	−1325.35188899	0.18
C-*R*-247	101.70	−170.50	−51.00	69.07	86.67	98.50	−46.98	142.71	110.99	70.87	172.91	−1325.35131606	0.54
C-*R*-248	96.77	−166.66	−48.97	67.20	−165.27	−168.20	67.84	−131.67	−81.27	59.94	106.32	−1325.34862475	2.23
C-*R*-249	98.61	−171.08	−49.55	72.36	−158.80	−51.98	−43.52	−76.09	−73.32	64.92	104.49	−1325.35217719	0.00
C-*R*-250	93.44	−173.16	−48.64	74.73	−169.46	−99.72	47.43	−141.85	−115.34	81.41	178.02	−1325.35170537	0.30
C-*R*-251	94.83	−172.31	−46.48	75.22	−176.68	−64.80	−40.31	173.62	114.99	78.04	176.41	−1325.34861944	2.23
C-*R*-258	100.47	−171.04	−53.00	65.92	86.99	−179.52	−63.40	113.39	72.09	71.84	−82.95	−1325.34987568	1.44
C-*R*-272	91.15	−172.13	−49.35	66.29	73.28	45.57	42.71	76.44	73.33	74.12	−102.79	−1325.34950697	1.68
C-*R*-273	92.65	−173.48	−49.65	73.96	171.88	60.28	41.82	−175.41	−113.63	71.78	−173.95	−1325.34784915	2.72

R-configuration carvedilol at the restricted Hartree−Fock (RHF/3-21G) level of theory. All calculations were performed using the Gaussian 98 (G98) software program and *R*-configuration carvedilol was fully structurally defined using the G98 Cartesian and *z*-matrix internal coordinate system to specify molecular structure, stereochemistry, and geometry.[19] Graphical data were plotted using Axum 5.0.[20]

3. Results and Discussion

3.1. Review of Converged Carvedilol Conformations. All 240 carvedilol input (i.e., predicted) structures (conformations C-*R*-1 to C-*R*-240 found in Table S1) were optimized at the RHF/3-21G level of theory. Consequently, this optimization process revealed a total of 121 unique carvedilol conformations with a range in relative conformer energy of ~23 kcal/mol (cf. Table S2 in the Supporting Information). However, not all of the 121 converged conformations were predicted from the fragment analysis; 35 novel conformations were revealed by optimization (indicated as conformations C-*R*-241 to C-*R*-275 in Tables S1 and S2). Thus, there was a convergence of 44% (121/275) for all carvedilol conformers evaluated. The input and optimized conformations of all carvedilol structures are found in Table S1, whereas all explicit optimized values and energies, as well as tabulations of conformers that moved to different parts of the PEHS and annihilated conformers, are displayed in Table S2.

As previously discussed in the literature,[4,7,14−18] and now shown for the first time in Table S2, the carvedilol PEHS possesses great and dramatic conformational flexibility. Carvedilol conformations converged at various points on the PEHS and numerous structures were able to move to both nearby and distant conformations from starting input orientations that did not converge. Although it was common for groups of structures with similar conformations to converge (cf. conformers C-*R*-55 to C-*R*-59, C-*R*-117[a] to C-*R*-119, and C-*R*-193 to C-*R*-204 in Table S2), it was also frequently observed that single conformations converged among portions of the PEHS that were scarcely populated and filled with large numbers of annihilated structures (cf. C-*R*-106, C-*R*-156, C-*R*-171, and C-*R*-184 in Table S2).

3.2. Structural Analysis of Carvedilol Low-Energy Conformers. To arrive at a set of low-energy conformers for the carvedilol PEHS, all converged conformations were plotted according to their respective relative energy (cf. Figure 3). The plot illustrates the inherent flexibility of the carvedilol molecule as converged conformations are dispersed over a large range of relative energies. However, there is a definitive set of nine low-energy conformations in the bottom right-hand corner of Figure 3; these conformations are bounded by a conformer relative energy of <4 kcal/mol and are clearly divided from the rest of the converged structures. These nine conformations include the following: C-*R*-246 to C-*R*-251, C-*R*-258, C-*R*-272, and C-*R*-273 (cf. molecular structures in Figure 4 and optimized parameters in Table 2).

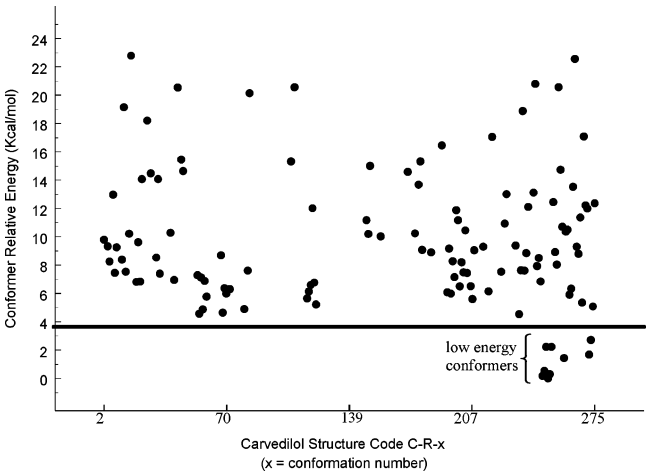

Figure 3. Conformer relative energies for all carvedilol structures optimized in the current study. The plot identifies a group of nine low-energy conformations in the bottom right-hand corner bounded by a relative conformer energy of <4 kcal/mol (cf. Table 2 and Figure 4 for the respective optimized parameters and structures of these low-energy conformers).

Close scrutiny of the low-energy conformations reveals a surprising finding: seven (C-*R*-246 to C-*R*-250, C-*R*-258, and C-*R*-272) of the nine conformations possess a distinctive common structural motif. These seven carvedilol structure are dominated by a "tetra-centric" (i.e., four-centered) conformation (cf. Figure 5). The tetra-centric conformation is flanked on one side (the "left side" of carvedilol) by the 13-membered aromatic carbazole ring (center 1), which is connected to a six-membered ring closed via an intramolecular O···H−N H-bond between the carbazole ether oxygen and a proton of the positive N atom of carvedilol (ring **a**; center 2). The same protonated secondary N atom forms an eight-membered ring (ring b; center 3) through another intramolecular O···H−N H-bond to the methoxy oxygen of carvedilol. The "right side" of the carvedilol conformation is flanked by the disubstituted benzene ring (center 4), which also forms part of ring **b**. Rings **a** and **b** are formed via short, strong H-bonds that are, in all cases, <2 Å long. Conformations C-*R*-251 and C-*R*-273 do not form any IMAF with the methoxy oxygen, O36, and, thus, do not form ring **b**.

The most striking feature of this tetra-centric conformation is the necessary protonated secondary nitrogen in the side chain of carvedilol. This positive nitrogen center is required for the concomitant formation of the two essential O···H−N H-bonds, because it would not be possible to form these two H-bonds, and, subsequently rings **a** and **b,** with a bifurcated H-bond involving only one amine proton. Moreover, the argument can

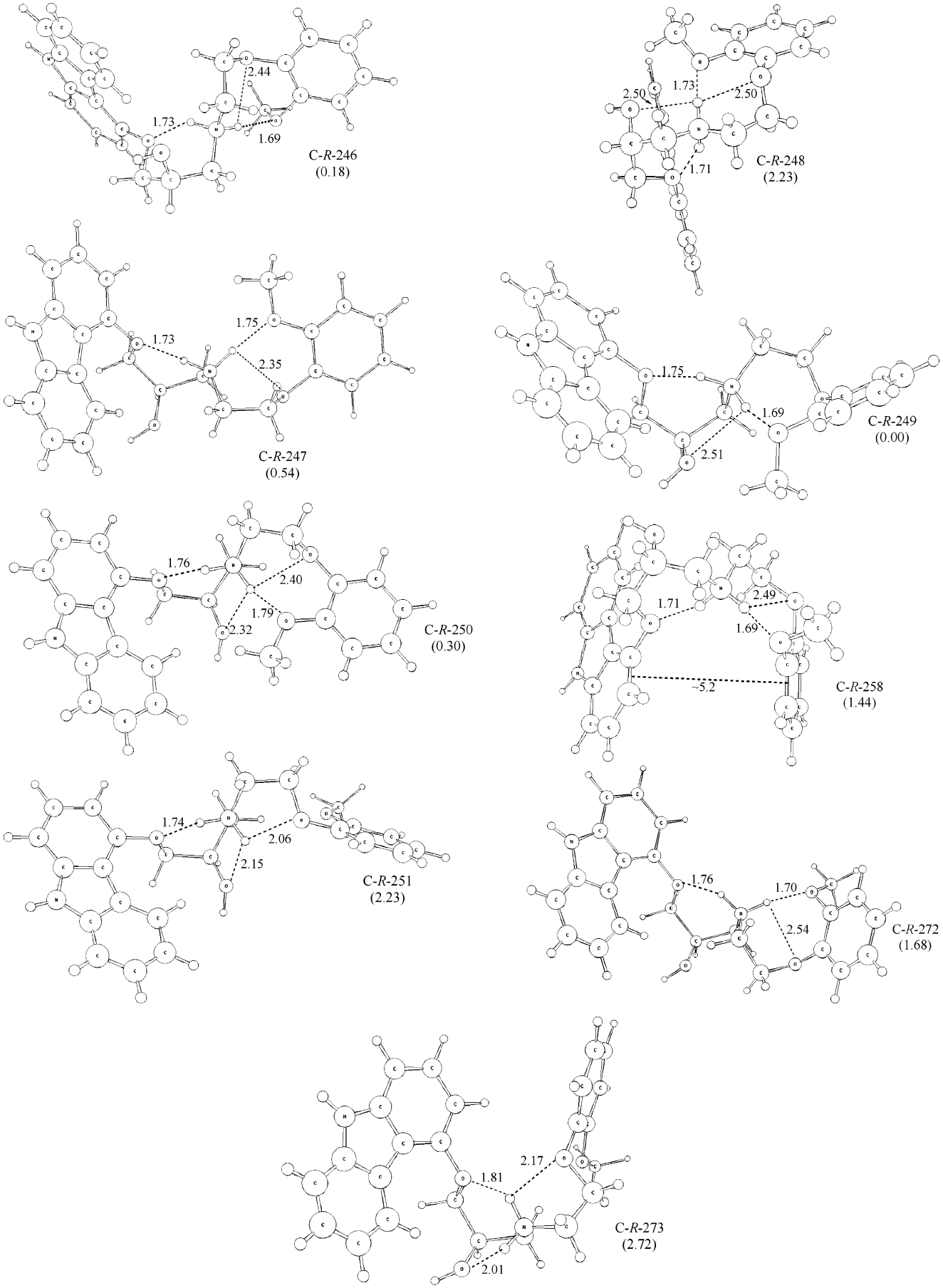

Figure 4. Molecular structures of the nine low-energy protonated carvedilol conformers revealed in the current study. Structures were fully optimized at the RHF/3-21G level of theory (relative energy for each structure is denoted in brackets; cf. Table 2 for optimized parameters).

be extended in that an electron-deficient N atom will be optimally stabilized by the formation of rings **a** and **b**, because this will allow better electron induction to the nitrogen center.

As far as we know, such a carvedilol conformation as shown in Figure 5 has not previously been presented or discussed in the literature. In the past, it has been postulated that internal hydrogen bonding between the ether carbazole oxygen, amine center, and catechol O atoms are dominant, but nonspecific, IMAFs of carvedilol.[4,7] We have earlier shown that such conformations do exist and the most significant intramolecular H-bond network is an O1···H42−O41···H57 double H-bond (left side), along with a bifurcated O29···H46···O36 H-bond (right side).[18] Therefore, this communication is the first instance of a specific carvedilol conformation that contains no such H-bond network present, because H42 does not hydrogen-bond with any other atoms in the tetra-centric structure (cf. Figures 4 and 5).

The torsional angle orientations basic for carvedilol to assume this tetra-centric conformation are shown in eq 5 (a forward slash ("/") indicates "or").

$$\chi_1 = g+ \tag{5a}$$

$$\chi_2 = a \tag{5b}$$

$$\chi_3 = g- \tag{5c}$$

$$\chi_4 = g+ \tag{5d}$$

$$\chi_5 = g+/a \tag{5e}$$

$$\chi_6 = g+/a/g- \tag{5f}$$

$$\chi_7 = g+/g- \tag{5g}$$

$$\chi_8 = g+/a/g- \tag{5h}$$

$$\chi_9 = g+/g- \tag{5i}$$

$$\chi_{10} = g+ \tag{5j}$$

$$\chi_{11} = g+/a/g- \tag{5k}$$

Although the carvedilol PEHS is one of large conformational flexibility, this tetra-centric conformation possess uncanny rigidity in that 5 (χ_1, χ_2, χ_3, χ_4, and χ_{10}) of the 11 torsional angles only assume one orientation. Because all five of these rigid torsional angles belong to Fragment A, it can thus be stated that it is the carbazole-containing pharmacophore that characterizes this prevalent and extremely stable conformation.

Upon closer investigation of the molecular structures in Figure 4, aside from the tetra-centric motif, converged conformations that possess further intramolecular H-bond networks are found, albeit these are composed of much longer H-bonds, compared to those of enclosed rings **a** and **b**. Aside from differences related to the tetra-centric conformational motif, the nine low-energy carvedilol structures can be divided into two groups: those with three internal H-bonds (C-*R*-246, C-*R*-247, C-*R*-249, C-*R*-251, C-*R*-258, C-*R*-272, and C-*R*-274) and those with four internal H-bonds (C-*R*-248 and C-*R*-250) (cf. Figure 4).

In the case of structures with three H-bonds, C-*R*-246 forms a five-membered ring via a 2.44 Å O29···H−N H-bond, whereas C-*R*-247 forms a similar five-membered ring with a 2.35 Å O29···H−N H-bond. The global minima C-*R*-249 forms a different five-membered ring with the hydroxyl oxygen (at the carvedilol stereocenter) through a 2.51 Å O41···H−N H-bond, whereas oxygen O29 does not partake in any specific IMAF. Conformer C-*R*-251 does not possess the tetra-centric motif (it lacks ring **b**) and forms a five-membered ring with a 2.15 Å O41···H−N H-bond and an additional five-membered ring via a 2.06 Å O29···H−N H-bond. Carvedilol structure C-*R*-258 forms a five-membered ring through a 2.49 Å O29···H−N H-bond and besides being described by the tetra-centric motif, its conformation resembles that of a "clam shell", where the two flanking aromatic centroids are separated by ∼5.2 Å. C-*R*-272 forms a five-membered ring with a 2.54 Å O29···H−N H-bond. Finally, conformer C-*R*-273 does not display the tetra-centric motif; instead, it is characterized by the same two five-membered rings displayed by the only other low-energy conformation that does not have the tetra-centric design (C-*R*-251): a five-membered ring with a 2.01 Å O41···H−N H-bond and a five-membered ring connected by a 2.17 Å O29···H−N H-bond.

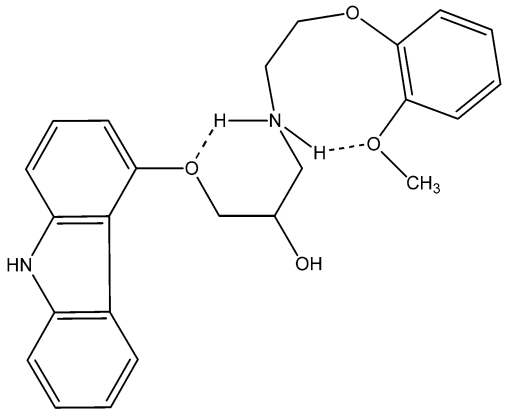

Figure 5. Schematic representation of the "tetra-centric" conformational motif exhibited by seven (C-*R*-246 to C-*R*-250, C-*R*-258, and C-*R*-272) of the nine carvedilol low-energy conformations (cf. Figure 4). This structural motif consists of a six-membered ring (ring **a**) bonded to the terminal carbazole centroid (left side of carvedilol) and an eight-membered ring (ring **b**) bonded to the terminal substituted benzene (right side of carvedilol); the rings are connected to each other via the protonated secondary nitrogen of carvedilol. The two intramolecular rings are formed by means of two (one in each ring) O···H−N hydrogen bonds (H-bonds) which, in all cases, are short H-bonds (<2 Å in distance). For carvedilol to form this structural motif, the following conformation is required: $\chi_1 = g+$, $\chi_2 = a$, $\chi_3 = g-$, $\chi_4 = g+$, $\chi_5 = g+/a$, $\chi_6 = g+/a/g-$, $\chi_7 = g+/g-$, $\chi_8 = g+/a/g-$, $\chi_9 = g+/g-$, $\chi_{10} = g+$, and $\chi_{11} = g+/a/g-$.

In regard to the two conformers with four internal H-bonds, C-*R*-248 and C-*R*-250, both possess the tetra-centric structure. Furthermore, C-*R*-248 possesses a five-membered ring with a 2.50 Å O41···H−N H-bond and another five-membered ring by means of a 2.50 Å O29···H−N H-bond. Conformer C-*R*-250 is similar to the latter structure with a five-membered ring via a 2.32 Å O41···H−N H-bond and a five-membered ring connected by a 2.40 Å O29···H−N H-bond. All low-energy conformations have double bifurcated H-bonds, although not all are the same, whereas conformers C-*R*-248 and C-*R*-250 assume an orientation with a triple H-bond bifurcation (the former and latter are relative to one amine proton).

3.3. Evaluation of Pharmacophore Fragmentation as a Method To Predict and Optimize Low-Energy Conformations of Carvedilol. As discussed previously in the Introduction, given carvedilol's varied and versatile pharmacological actions and multifaceted pharmacodynamic and therapeutic nature, it is exceptionally relevant to examine carvedilol's complete molecular identity at the fundamental level of conformation. Elucidation of carvedilol's conformational identity should

TABLE 3: Summary of the Conformation Distribution for Optimized Low-Energy Carvedilol Conformations (cf. Table 2) and Optimized Low-Energy Fragment Conformations Used To Make Carvedilol Conformation Predictions (cf. Table 1)[a]

Conformation Distribution of Optimized Carvedilol Low-Energy Conformers (cf. Table 2)[b]			
torsional angle	*g*+	*a*	*g*−
χ_1	**9/9 (100%)**	(0%)	(0%)
χ_2	(0%)	**9/9 (100%)**	(0%)
χ_3	(0%)	(0%)	**9/9 (100%)**
χ_4	**9/9 (100%)**	(0%)	(0%)
χ_5	4/9 (44.4%)	**5/9 (55.6%)**	(0%)
χ_6	3/9 (33.3%)	3/9 (33.3%)	3/9 (33.3%)
χ_7	4/9 (44.4%)	(0%)	**5/9 (55.6%)**
χ_8	2/9 (22.2%)	**5/9 (55.6%)**	2/9 (22.2%)
χ_9	4/9 (44.4%)	(0%)	**5/9 (55.6%)**
χ_{10}	9/9 (100%)	(0%)	(0%)
χ_{11}	3/9 (33.3%)	**4/9 (44.4%)**	2/9 (22.2%)
Conformation Distribution of Initial Optimized Low-Energy Carvedilol Fragments (cf. Table 1)[c]			
fragment	*g*+	*a*	*g*−
	(0%)	3/4 (75%)	1/4 (25%)
A	(0%)	**3/4 (75%)**	1/4 (25%)
	(0%)	3/4 (75%)	**1/4 (25%)**
	3/8 (37.5%)	5/8 (62.5%)	(0%)
B	2/8 (25%)	**6/8 (75%)**	(0%)
	3/8 (37.5%)	3/8 (37.5%)	2/8 (25%)
	3/6 (50%)	(0%)	**3/6 (50%)**
C	2/6 (33.3%)	**2/6 (33.3%)**	2/6 (33.3%)
	3/6 (50%)	(0%)	**3/6 (50%)**
A	**3/4 (75%)**	(0%)	1/4 (25%) FA
B	**8/8 (100%)**	(0%)	(0%)
C	N/A	N/A	N/A
C	2/6 (33.3%)	**2/6 (33.3%)**	2/6 (33.3%)

[a] The dominant torsional angle conformation for carvedilol and the corresponding fragment conformation is given in bold type, for ease of comparison. (Legend is as follows: FA, Fragment A; FB, Fragment B; FC, Fragment C; and N/A, not applicable.) [b] In regard to the nine carvedilol low-energy converged structures, the conformation distribution is displayed as the number of conformations, with the respective torsional angle orientation/total number (i.e., nine) of conformations (corresponding percentage is indicated in parentheses). [c] In regard to the low-energy carvedilol fragment structures, the conformation distribution is displayed as the number of conformations, with the respective torsional angle orientation/total number of conformations (corresponding percentage is indicated in parentheses). Note that the total number of conformations is dependent on how many fragment structures were found to possess a conformer relative energy of ≤2.00 kcal/mol and, thus, is different for each fragment (Fragment A has four conformations, Fragment B has eight conformations, and Fragment C has six conformations).

greatly aid further molecular understanding of carvedilol's adrenoceptor binding conformation and its amelioration in pathological states such as oxidative stress (through inhibition of ROS) and AD (as an antifibrillar agent). Nonetheless, given the current cost of computer processing power and the fact that carvedilol's PEHS possesses an exorbitant number of conformational possibilities ($3^{11} = 177\,147$ conformational possibilities), traditional MDCA approaches to solving its PEHS are daunting and unfeasible. In reality, the problem of solving carvedilol's PEHS is analogous to the difficulties encountered in deciphering complete conformational profiles for any medium- to large-sized molecular system, such as drug molecules and proteins with large degrees of freedom.

The current authors have sought to circumvent the problem of solving carvedilol's conformations by creating a method in which carvedilol was divided into three molecular fragments, according to pharmacophore structure−activity, and each fragment was optimized with MDCA (cf. Figures 1 and 2). The results from previous studies were used here to predict possible conformations of carvedilol based on the idea that, because only low-energy fragment conformations would be used, these would ultimately lead to the discovery and optimization of low-energy conformations for the entire carvedilol molecule. After having performed the aforementioned tasks, it is vital to evaluate the success of this novel approach; this evaluation addresses both the accuracy and overall usefulness (i.e., utility and expediency) of this method.

Superficially, given that all nine low-energy conformations (cf. Table 2) are described by conformational assignments not predicted by the individual fragment analysis, it would seem that such a method was not able to predict the low-energy conformations of carvedilol accurately. All low-energy conformations for carvedilol comprise a *g*+ orientation for torsional angle χ_1, whereas no Fragment A low-energy structure (≤2 kcal/mol) had this orientation. Instead, Fragment A conformers with $\chi_1 = g+$ possessed conformer relative energies of 2.26, 5.11, and 6.34 kcal/mol (cf. ref 17). Because the lowest energy of these conformers was greater than the 2 kcal/mol threshold applied, it was not included as a low-energy fragment structure and, thus, was not utilized to predict carvedilol conformations. However, this in itself does not invalidate the accuracy of this methodology, because a distinct set of low-energy conformers were ultimately discovered and optimized. Because of this issue, it is necessary to look closer at the predicted conformations generated and the low-energy structures discovered.

To compare the predictions and eventual optimized results in depth, the conformation distribution for each torsional angle for the optimized results (taken from Table 2) and the initial predicted conformation (taken from Table 1) must be noted (cf. Table 3). Upon inspection and comparison, we see that the conformation distribution of 8 (χ_2, χ_5, χ_6, χ_7, χ_8, χ_9, χ_{10}, and χ_{11}) of the 11 torsional angles were accurately predicted (72.7%). Given this assessment, one can deem the accuracy of this method as satisfactory. The reason all nine of the low-energy conforma-

tions were not present in our predictions involved our inability to predict the conformation of torsional angles χ_1, χ_3, and χ_4, which were essentially localized in one torsional angle orientation for all low-energy conformations; the latter allows the formation of the tetra-centric structural motif. It is postulated that the inability to predict these torsional angles results from the fact that Fragment A only had a terminal methyl group for χ_4, and, therefore, the complexity of this section of the carvedilol structure could not be fully described. Even so, the accuracy of this method is satisfactory, because the inability to predict some conformation distributions was compensated by a high degree of prediction in other torsional angles such as χ_2, χ_5, χ_7, χ_9, and χ_{10} (cf. Table 3). The final result is that this method of evaluation allowed us not only to find a defined set of low-energy carvedilol conformers upon optimization of predicted inputs, but also to reveal a novel structural motif.

In regard to utility and expediency, it is clear that the current fragmentation method has greatly aided the problem of deciphering the low-energy conformations of carvedilol. This is to say, the robustness of this methodological approach allowed us to take an exhaustive PEHS and convert it to a series of smaller, well-defined, and more-manageable conformational surfaces, while retaining some major properties of the entire system in each fragment. Although such a method has obvious shortcomings, it is able to achieve its overall objectives and goals.

As theoretical and computational methods move progressively into the realm of larger molecular systems, certain workers have emphasized the need for studies to find ever-evolving methods, rather than relying on brute computing force, to evaluate every possible conformation of such complicated systems effectively.[21] These methods will likely rely on the ability to sample portions of a PEHS as a means to arrive at the significantly populated conformations; in other words, the challenge of sampling conformations is to ensure that one is able to ultimately consider the most populated and significant states because, according to basic thermodynamics, only low-energy states will be significantly occupied.[21] It has been previously postulated that the success of such novel methodological approaches to finding the dominant conformations of large PEHSs via sampling will be dependent on the ability of these methods to generate starting points (on portions of a PEHS) with some amount of energy minimization.[21] This will allow investigators to efficiently realize which portions of a PEHS they should focus on.

The fragmentation methodology used in this study achieves the goal described previously, because the carvedilol map is not sampled randomly in an attempt to discover highly populated low-energy states. Rather, the carvedilol fragments are optimized to generate inputs (i.e., from low-energy optimized fragment conformations) with an inherent amount of energy minimization/optimization. This methodological standpoint greatly simplifies sampling a large PEHS such as that of carvedilol's, because it is oriented to hypothesized low-energy conformers.

4. Conclusions

In the current study, a set of gas-phase low-energy carvedilol conformations have been evaluated and presented; 240 carvedilol conformers were initially optimized, revealing 121 converged structures. Using a rational molecular fragmentation method, nine converged low-energy conformations were discovered, seven of which possessed a unique "tetra-centric" (four-centered) conformational motif not previously encountered in the literature. Further evaluation of these conformations, by means of optimizations and structural analysis at high-level, electron-correlated model chemistries is currently being conducted. Furthermore, optimization of these nine low-energy conformers in the solvent phase, and not merely single-point-energy (SPE) calculations, will greatly benefit the characterization of the magnitude of a solvent effect on these carvedilol conformations. With respect to further evaluation of the molecular fragmentation method used here, experimental analysis of carvedilol conformations, such as that with nuclear magnetic resonance (NMR) spectroscopy, would allow full comparison between the theoretically and experimentally determined carvedilol structures. Together, this will lead to the solution of the dominant conformations of carvedilol that is expected to dominate gas- and solvent-phase samples, which, in turn, will further expound carvedilol's molecular profile and pharmacodynamic attributes.

Acknowledgment. One of the authors (I.G.C.) would like to thank the Hungarian Ministry of Education for a Szent-Györgyi Visiting Professorship.

Supporting Information Available: List of all unique carvedilol conformations generated from the combination of low-energy conformers in Table 1 and the conformation of subsequently optimized structures (Table S1, PDF) and optimized values for the converged conformers of the protonated carvedilol surface at the RHF/3-21G level of theory (Table S2, PDF). This material is available free of charge via the Internet at http://pubs.acs.org.

References and Notes

(1) Cheng, J.; Kamiya, K.; Kodama, I. *Cardiovasc. Drug Rev.* **2001**, *19*, 152.

(2) Carlson, W.; Oberg, K. *J. Cardiovasc. Pharmacol. Ther.* **1999**, *4*, 205.

(3) Capomolla, S.; Febo, O.; Gnemmi, M.; Riccardi, G.; Opasich, C.; Carporotondi, A.; Mortara, A.; Pinna, G.; Cobelli, F. *Am. Heart J.* **2000**, *139*, 596.

(4) Oliveira, P. J.; Marques, M. P.; Batista de Carvalho, L. A. E.; Moreno, A. J. M. *Biochem. Biophys. Res. Commun.* **2000**, *276*, 82.

(5) Tzagoloff, A. *Mitochondria*; Plenum Press: New York, 1982.

(6) Korshunov, S. S.; Skulachev, V. P.; Starkov, A. A. *FEBS Lett.* **1997**, *416*, 15.

(7) Howlett, D. R.; George, A. R.; Owen, D. E.; Ward, R. V.; Markwell, R. E. *Biochem. J.* **1999**, *343*, 419.

(8) Hardy, J.; Selkoe, J. *Science* **2002**, *297*, 353.

(9) Lee, V. M.-Y. *Neurobiol. Aging* **2002**, *23*, 1039.

(10) Walsh, D. M.; Klyubin, I.; Fadeeva, J. V.; Cullen, W. K.; Anwyl, R.; Wolfe, M. S.; Rowan, M. J.; Selkoe, D. J. *Nature* **2002**, *416*, 535.

(11) Lambert, M. P.; Barlow, A. K.; Chromy, B. A.; Edwards, C.; Freed, R.; Liosatos, M.; Morgan, T. E.; Rozovsky, I.; Trommer, B.; Viola, K. L.; Wals, P.; Zhang, C.; Finch, C. E.; Krafft, G. A.; Klein, W. L. *Proc. Natl. Acad. Sci. U.S.A.* **1998**, *95*, 6448.

(12) Walsh, D. M.; Hartley, D. M.; Kusumoto, Y.; Fezoui, Y.; Condron, M. M.; Lomakin, A.; Benedek, G. B.; Selkoe, D. J.; Teplow, D. B. *J. Biol. Chem.* **1999**, *274*, 25945.

(13) Chui, D.-H.; Tanahashi, H.; Ozawa, K.; Ikeda, S.; Checler, F.; Ueda, O.; Suzuki, H.; Araki, W.; Inoue, H.; Shirotani, K.; Takahashi, K.; Gallyas, F.; Tabira, T. *Nature Med.* **1999**, *5*, 560.

(14) Almeida, D. R. P.; Pisterzi, L. F.; Chass, G. A.; Torday, L. L.; Varro, A.; Papp, J. Gy.; Csizmadia, I. G. *J. Phys. Chem. A* **2002**, *106*, 10423.

(15) Almeida, D. R. P.; Gasparro, D. M.; Pisterzi, L. F.; Torday, L. L.; Varro, A.; Papp, J. Gy.; Penke, B. *J. Mol. Struct. (THEOCHEM)* **2003**, *631*, 251.

(16) Almeida, D. R. P.; Gasparro, D. M.; Pisterzi, L. F.; Juhasz, J. R.; Fülöp, F.; Csizmadia, I. G. *J. Mol. Struct. (THEOCHEM)* **2003**, *666*−*667*, 557.

(17) Almeida, D. R. P.; Gasparro, D. M.; Pisterzi, L. F.; Torday, L. L.; Varro, A.; Papp, J. Gy.; Penke, B.; Csizmadia, I. G. *J. Phys. Chem. A* **2003**, *107*, 5594.

(18) Almeida, D. R. P.; Gasparro, D. M.; Pisterzi, L. F.; Juhasz, J. R.; Fülöp, F.; Csizmadia, I. G. *J. Mol. Struct. (THEOCHEM)* **2003**, *666*−*667*, 537.

(19) Frisch, M. J.; Trucks, G. W.; Schlegel, H. B.; Scuseria, G. E.; Robb, M. A.; Cheeseman, J. R.; Zakrzewski, V. G.; Montgomery, J. A., Jr.; Stratmann, R. E.; Burant, J. C.; Dapprich, S.; Millam, J. M.; Daniels, A. D.; Kudin, K. N.; Strain, M. C.; Farkas, O.; Tomasi, J.; Barone, V.; Cossi, M.; Cammi, R.; Mennucci, B.; Pomelli, C.; Adamo, C.; Clifford, S.;

Ochterski, J.; Petersson, G. A.; Ayala, P. Y.; Cui, Q.; Morokuma, K.; Malick, D. K.; Rabuck, A. D.; Raghavachari, K.; Foresman, J. B.; Cioslowski, J.; Ortiz, J. V.; Stefanov, B. B.; Liu, G.; Liashenko, A.; Piskorz, P.; Komaromi, I.; Gomperts, R.; Martin, R. L.; Fox, D. J.; Keith, T.; Al-Laham, M. A.; Peng, C. Y.; Nanayakkara, A.; Gonzalez, C.; Challacombe, M.; Gill, P. M. W.; Johnson, B. G.; Chen, W.; Wong, M. W.; Andres, J. L.; Head-Gordon, M.; Replogle, E. S.; Pople, J. A. *Gaussian 98*, revision A.9; Gaussian, Inc.: Pittsburgh, PA, 1998.

(20) *Axum 5.0C for Windows*; MathSoft Incorporated, 1996.

(21) Billings, E. Molecular Modeling and Drug Design. In *Foye's Principles of Medicinal Chemistry*, 5th ed.; Williams, D. A., Lemke, T. L., Eds.; Lippincott Williams & Wilkins: New York, 2002; pp 68−85.